



Nicolae Digă , Constantin Ghiță , Silvia-Maria Digă , Dorinel Constantin,
Maria Brojboiu

Application of Finite Element Method to Determine the Performances of a Permanent Magnet Synchronous Motor for Driving a Bicycle

In this paper, the authors present a case study in which was analyzed by finite element method a permanent magnet synchronous motor for driving a bicycle using the analysis and simulation software ANSYS Electromagnetics Low Frequency of ANSYS Inc. Company. Modelling and simulation with ANSYS[®] Maxwell 2D of electromagnetic field in the studied motor was conducted for different initial positions (internal angle rotor-stator configured (set)) θ_1 . It was identified the internal angle for which the performances of PMSM are very close to those obtained by computation.

Keywords: AC motor drives, electromagnetic fields, finite element methods, permanent magnet motors, software packages.

1. Introduction

The study of the permanent magnet synchronous motor for driving a bicycle from electromagnetic point of view is presented below. For this purpose, the finite element method was applied.

The computations are based on the finite element method in 2D approximation, the results being useful in optimal design of the permanent magnet synchronous machines. The numerical investigations presented in this paper are based on Finite Element Method (FEM) implemented in ANSYS[®] software packages (RMxpert, Maxwell 2D, Maxwell 3D) [1], [6].

The permanent magnet synchronous motors (PMSM) are extensively used for the electric drive systems [2]-[4]. The main advantages are the high efficiency and

power factor, stable and reliable operation and no required additional dc excitation source [7].

2. The studied motor description

The machine is a permanent magnet synchronous motor, three phases with the following characteristics: rated power 500 W, rated voltage $3 \times 36 / 3$ V (stator star connexion), rated speed 130.434 rpm, rated frequency 50 Hz. The analyzed permanent magnet synchronous motor has 23 pole pairs on the rotor and 51 stator slots. A cross-section of the motor under study is shown in the Figure 1. The permanent magnets of the PMSM are sintered R1 type, with the return coefficient $\sim_r = 1.05$ and the remanent magnetic flux density $B_r = 0.7$ T, unidirectional magnetized.

Regarding the motor construction, the rotor is made cylindrical and radial air gap. The ferromagnetic armatures length is $l_r = 24$ mm (rotor), $l_s = 23.529$ mm (stator) and the air gap length is $g = 1$ mm.

The number of stator slots ($Z_s = 51$) and the number of poles ($2p = 46$) of permanent magnet synchronous motor were chosen to obtain a low value (1 in our case) of the greatest common divisor, as it is noticed in Figure 1. By this measure we ensure that permanent magnet synchronous motor produces very low value of the cogging torque, which is an important factor for any synchronous motor. The cogging torque has only the undesirable effects on synchronous motors namely: noises and vibrations which lead to the increased mechanical losses, the increased breaks (cutting) of the bicycle speed, the superior harmonics in the electromotive waveform, the mechanical imbalance to the shaft etc. [5], [7].

The PMSM which is studied in this paper has the trapezoidal slots with rounded corners and the stator teeth with parallel walls. The three phase stator windings are made from 51 coils (102 sides), 17 coils (34 sides) per phase. Each coil (side) has an aperture of a tooth (this is the tooth winding) as is shown in Figure 1, in each stator slot being placed two coil sides. The stator winding has a special structure, with a fractional number of slots per pole and phase q , whose expression is given by the formula:

$$q = \frac{Z_s}{2m_1p} = \frac{51}{2 \cdot 3 \cdot 23} = 0.3695, \quad (1)$$

where: Z_s - number of stator slots; m_1 - number of phases; p - number of pole pairs of the motor.

The elements of stator winding (armature) are detail presented in [4]. The magnetic core of stator is made from magnetic steel sheets type M19_24G_2DSF0.969 and the magnetic core of rotor is made from usual cast steel with magnetic properties weaker than the stator laminations, M19_24G_2DSF0.950.

3. Hardware and software support used

The software support is materialized in the "ANSYS Electromagnetics Low Frequency" made by ANSYS Inc. Company and provides the most efficient electromagnetic field analysis tools, used mainly for electric machines and equipment.

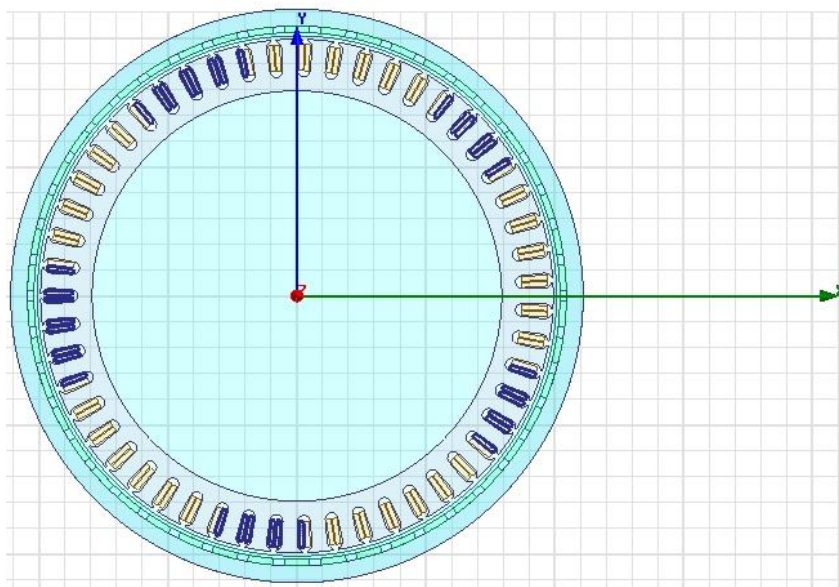


Figure 1. The motor geometry - cross-section [4]: 51 teeth; $t_{zs}=12.258$ mm - tooth pitch, $b_{zs}=5.895$ mm - tooth width, $B_{s0}=2$ mm - slot isthmus opening, $b_m=13$ mm - permanent magnet width.

The following products ANSYS Electromagnetics LF [1], [6]: ANSYS® Maxwell and ANSYS® RMXprt were used in this study.

3. 1. The RMXprt analysis results

Using the analytic classical theory of motors and the methods of equivalent magnetic circuits, ANSYS RMXprt can calculate the machine performances and make recommendations regarding to the initial dimensions.

The software generates as interfaces the results of the simulation performed on the motor (performances, design complete data, curves).

The interface which contains the motor performances that will be the input data for the subsequent analysis of electromagnetic field performed is shown in the Figure 2. The simulation is achieved so in the operation regime of maximum load and in the no-load regime.

The software generates customized interfaces for the permanent magnet, the rotor parameters and the stator parameters such as: the slots, the teeth, the winding and the steady-state parameters (Figure 3). The curves generated by the software are the following: the efficiency variation depending on the speed, $\eta = f(n)$; the useful power variation depending on the speed, $P_2 = f(n)$; the torque variation depending on the speed, $M = f(n)$; the cogging torque variation in two teeth depending on the speed, $T_{cog} = f(n)$; the variation of the induced voltages in a coil at the rated speed, depending on the electrical angle; the variation of the air-gap magnetic flux density depending on the electrical angle, $B = f(\theta)$; the variation of phase voltage induced in winding at the rated speed, depending on the electrical angle; the variation of currents (phase and line) in winding at load, depending on the electrical angle; the variation of phase voltage at load, depending on the electrical angle.

Data:

	Name	Value	Units	Description
1	Stator Winding Factor	0.943778		
2	D-Axis Reactive Inductance Lad	0.19765	mH	
3	Q-Axis Reactive Inductance Laq	0.19765	mH	
4	D-Axis Inductance L1+Lad	1.18103	mH	
5	Q-Axis Inductance L1+Laq	1.18103	mH	
6	Armature Leakage Inductance L1	0.98338	mH	
7	Zero-Sequence Inductance L0	0.805188	mH	
8	Armature Phase Resistance R1	0.504379	ohm	
9	D-Axis Time Constant	0.000391868	s	
10	Q-Axis Time Constant	0.000391868	s	
11	Ideal Back-EMF Constant KE	1.10319		Vs/rad.
12	Start Torque Constant KT	1.10317		Nm/A.

Figure 2. RMXprt interface - performances simulation - input data analysis with finite element method

3. 2. The modelling and simulation with ANSYS ® Maxwell 2D of electromagnetic field in the PMSM

ANSYS Maxwell uses the finite element method (FEM) to solve analyses with static fields, in the domain of variable frequency and time for electromagnetic and electric fields. A key element in ANSYS Maxwell is the possibility of generating

high-fidelity models and use of symmetry conditions in order to reduce solving time. Afterwards the project may be transferred in ANSYS Maxwell (2D/3D), where the materials, boundary conditions will be defined including here and symmetry cases, excitations and being coupled with circuits' topology to achieve an electro-magnetic analysis variable in time requested by a complex process of multi-criteria optimization.

Data:

	Name	Value	Units	Description
1	Stator Winding Factor	0.943778		
2	D-Axis Reactive Inductance Lad	0.19765	mH	
3	Q-Axis Reactive Inductance Laq	0.19765	mH	
4	D-Axis Inductance L1+Lad	1.18103	mH	
5	Q-Axis Inductance L1+Laq	1.18103	mH	
6	Armature Leakage Inductance L1	0.98338	mH	
7	Zero-Sequence Inductance L0	0.805188	mH	
8	Armature Phase Resistance R1	0.504379	ohm	
9	D-Axis Time Constant	0.000391868	s	
10	Q-Axis Time Constant	0.000391868	s	
11	Ideal Back-EMF Constant KE	1.10319		Vs/rad.
12	Start Torque Constant KT	1.10317		Nm/A.

Figure 3. RMXprt interface - steady-state parameters (permanent regime)

In the post-processing stage, the software generates the variation in time of several parameters: the variation of currents (phase and line) in winding depending on time; the developed torque variation depending on time, $M=f(t)$ (Figure 4); the iron (core) losses variation depending on time; the magnetic flux density distribution (diagram) depending on time (Figure 5); the distribution (spectrum) of the field lines depending on time; the vector magnetic potential distribution depending on time; the distribution of forces on the edges depending on time.

3. 3. Modelling and simulation with ANSYS ® Maxwell 3D of electromagnetic field in the PMSM

By using this software we can obtain both the whole model which can be viewed in Figure 6 but we can select also different regions of the motor as needed (the ensemble rotor - permanent magnets - air-gap - stator - shaft; the ensemble rotor - air-gap - stator; stator, etc.). The software generates also the scheme of the power supply circuit of the motor (inverter + command inverter + motor parameterized model).

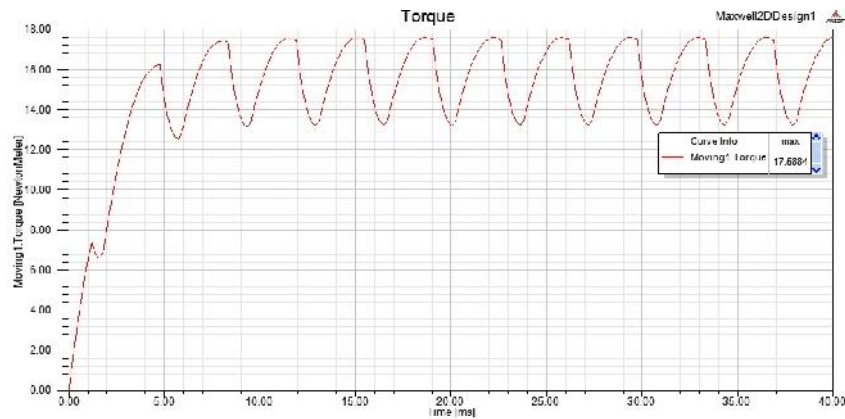


Figure 4. The developed torque variation depending on time, $M=f(t)$

The software also generates a set of curves: the variation of input dc current (command) of inverter depending on speed; the efficiency variation depending on speed, $\eta = f(n)$; the developed output (useful) power variation depending on speed, $P_2=f(n)$; the developed torque variation depending on speed, $M=f(n)$ (Figure 7); the variation of cogging torque depending on angle (Figure 8); the variation of voltage on a conductor, depending on angle; the variation of voltage on a turn, depending on angle; the variation of magnetic flux density in air-gap depending on angle; the variation of voltage (phase and line) induced in winding, depending on angle (Figure 9); the variation of currents (phase and line) provided by the power supply source, depending on angle.

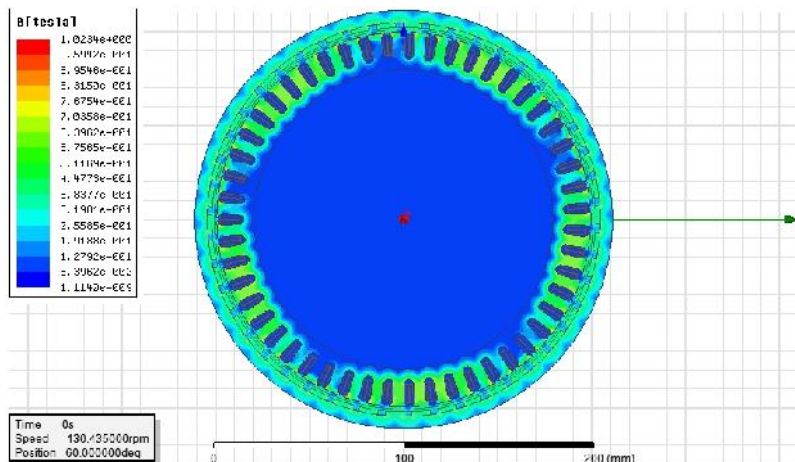


Figure 5. The magnetic flux density distribution (diagram) depending on time - Maxwell 2D interface

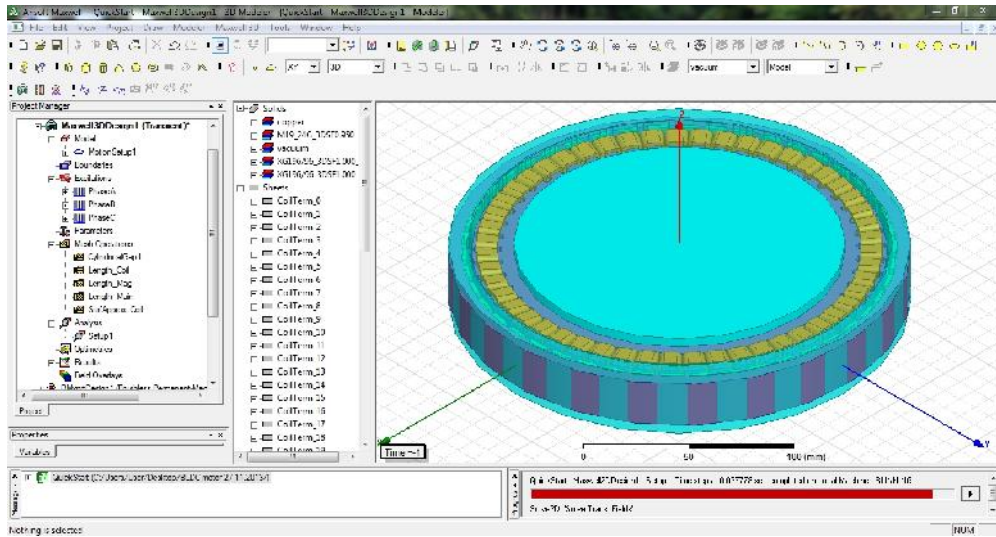


Figure. 6. The 3D model generated in transient regime of the motor - Maxwell 3D interface

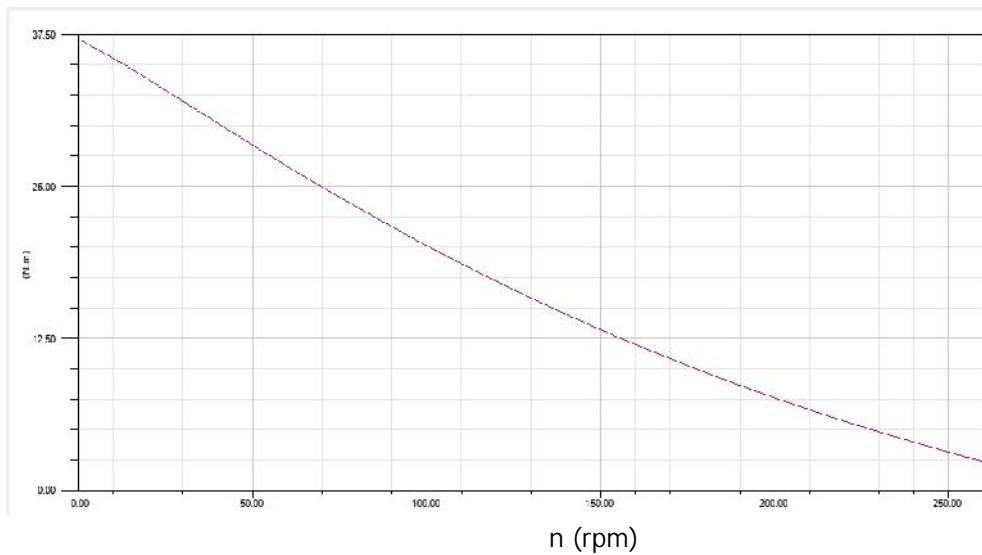


Figure. 7. The developed torque variation depending on speed, $M=f(n)$ - Maxwell 3D interface

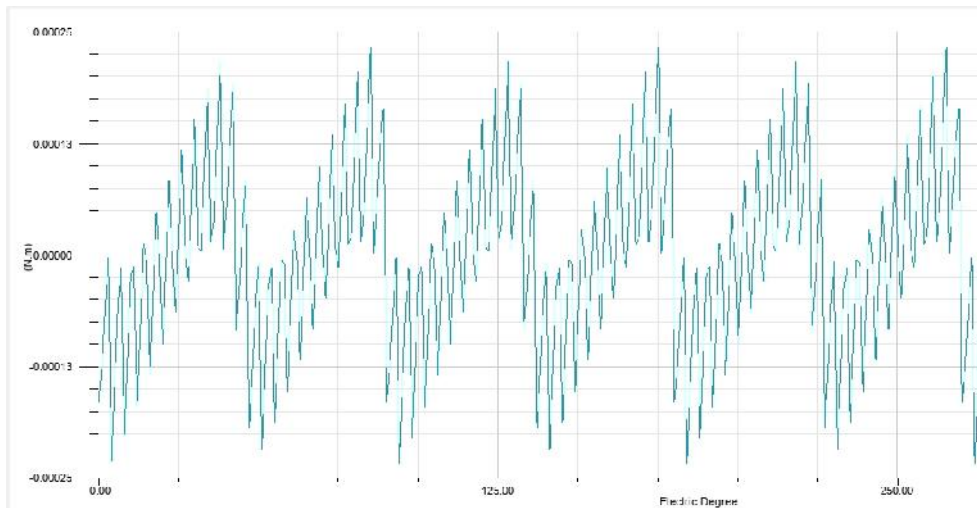


Figure. 8. The variation of cogging torque depending on angle - Maxwell 3D interface

4. Conclusion

The modelling and simulation with ANSYS ® Maxwell 2D of the electromagnetic field in the studied motor were conducted for different initial positions (internal angle rotor-stator configured $\alpha_1=4.3734^\circ$ and respectively $\alpha_2=60^\circ$). Consequently the major differences regarding the analyzed parameters were observed.

Thus it was found that at the steady state operation, the parameters values obtained by simulation for the initial position $\alpha_1=4.3734^\circ$ presented in Figure 3 and Table 1 are much closer than those obtained using the computing program developed in Mathcad, own conception which allowed the designing of the studied motor which is described in [3].

As subsequent research direction, based on the results within the presented simulations in this paper, will be achieved an analysis on this permanent magnet synchronous motor regarding the influence of the cross-section geometry of the motor, respectively the influence of the material properties on the useful magnetic flux.

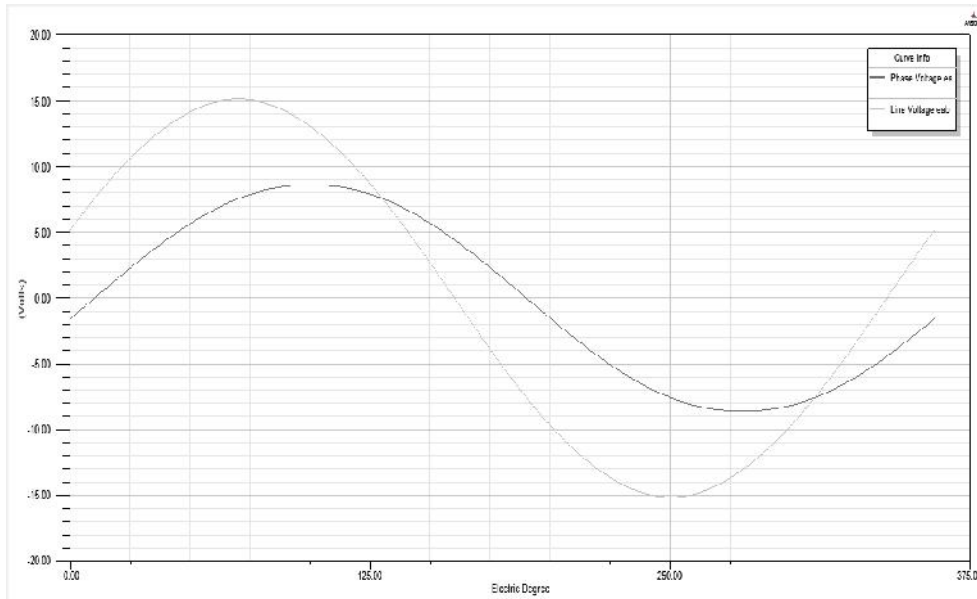


Figure. 9. The variation of the voltage (phase and line) induced in winding, depending on angle – Maxwell 3D interface

Table 1. Comparison between computed and simulated steady state parameters of the PMSM

Steady state parameters	Computation	Simulation, $\omega_1=4.3734^0$
Stator slot fill factor, k_{uc}	0.75	0.74033
D-Axis Inductance, L_d [mH]	2.7031	1.18103
Q-Axis Inductance, L_q [mH]	2.7031	1.18103
Armature leakage inductance, L_1 [mH]	0.97339	0.98338
Armature phase resistance, R_1 [Ω]	0.7182	0.504379
Estimated rotor moment of inertia, J_r [kg·m ²]	0.0114	0.0314407
Start torque constant, K_T [Nm/A]	1.7985	1.10317

References

- [1] **** Ansys-Ansoft 13, User' guide, 2008, ansoft-corporation.software.informer.com
- [2] Craiu O., **Contribuții privind metodele numerice de calcul al câmpului electromagnetic în mașinile electrice**, Teză de doctorat, Universitatea Politehnica din București, 1996.
- [3] Dig N., **Proiectarea și modelarea numerică 2D a motorului sincron cu magneți permanenți, pentru antrenarea unei biciclete**, Raport de cercetare nr. 1, coala doctorală Inginerie electrică, Universitatea Politehnica din București, 20 Iunie 2013.
- [4] Dig N., **Aplicarea metodei elementului finit pentru determinarea câmpului electromagnetic dintr-un motor sincron cu magneți permanenți, pentru antrenarea unei biciclete**, Raport de cercetare nr. 2, coala doctorală Inginerie electrică, Universitatea Politehnica din București, 13 Decembrie 2013.
- [5] Ghiță C., Nedelcu S., Trifu I., Tudorache T., **Finite Element Analysis of the Useful Magnetic Flux of a Low Speed PMSG**, University Politehnica of Bucharest, Scientific Bulletin, 2009.
- [6] **** INAS S.A., <http://www.inas.ro/>
- [7] Melcescu L., **Contribuții la studiul câmpului magnetic în mașinile sincrone cu magneți permanenți**, Teză de doctorat, Universitatea Politehnica din București, 2002.

Addresses:

- Drd. Eng. Nicolae Digă, Doctoral School of Electrical Engineering, University "Politehnica" of Bucharest, 313, Splaiul Independenței, Sector 6, 060042 Bucharest, nicolae.diga@yahoo.ro
- Prof. Dr. Eng. Constantin Ghiță, University "Politehnica" of Bucharest, 313, Splaiul Independenței, Sector 6, 060042 Bucharest, ghita.constantin@gmail.com
- Prof. Dr. Eng. Silvia-Maria Digă, University of Craiova, Faculty of Electrical Engineering, 107, Decebal Boulevard, Craiova, 200440, sdiga@elth.ucv.ro
- Drd. Eng. Dorinel Constantin, SC INAS SA, CAE Department, 37C, Nicolae Romanescu Str., Craiova, 200738, dconstantin@inas.ro
- Prof. Dr. Eng. Maria Brojboiu, University of Craiova, Faculty of Electrical Engineering, 107, Decebal Boulevard, Craiova, 200440, mbrojboiu@elth.ucv.ro